ELSEVIER

International Journal of Pharmaceutics 199 (2000) 167–177

international journal of pharmaceutics

www.elsevier.com/locate/ijpharm

Characterisation of a novel solid lipid nanoparticle carrier system based on binary mixtures of liquid and solid lipids

Volkhard Jenning [a], Andreas F. Thünemann [b], Sven H. Gohla [a,*]

[a] *Department of Pharmaceutics, Biopharmaceutics and Biotechnology, Free University of Berlin, Kelchstrasse 31, D-12169 Berlin, Germany*

[b] *Max-Planck-Institute of Colloidals and Interfaces, Potsdam, Germany*

Received 21 October 1999; received in revised form 1 February 2000; accepted 14 February 2000

Abstract

A drug carrier of colloidal lipid particles with improved payloads and enhanced storage stability was investigated. Based on the experiences with hard fats nanoparticles, a new type of solid lipid nanoparticles (SLN) has been developed by incorporating triglyceride containing oils in the solid core of said particle. The structure and mixing behaviour of these particles were characterised and practical implications on controlled release properties tested. Nanoparticles were characterised by their melting and recrystallisation behaviour as recorded by differential scanning calorimetry (DSC). Polymorphic form and bilayer arrangement were assigned by wide-angle X-ray scattering (WAXS) and small-angle X-ray scattering (SAXS). Size distribution and storage stability were investigated by laser diffractometry (LD). Release properties were studied by drug release model according to Franz. A medium chain triglyceride oil was incorporated successfully in a matrix of a solid long chain glyceride. The crystal order was greatly disturbed, however, the carrier remained solid. The oil inside the particle remained in a liquid state and induced a slight shift form the β' polymorph to the β_i form. Long spacings varied within 0.1 nm with increasing oil loads. Nanoparticles with low oil concentrations showed sustained release properties. Improved drug load levels were encapsulated by lipid particles supplemented with oily constituents. Thus, the presented carrier adds additional benefits to the well-known opportunities of conventional SLN and is suited for topical use.

Keywords: Solid lipid nanoparticles; Loading capacity; Crystal order; Physical stability; Drug release

1. Introduction

Solid lipid nanoparticles (SLN) based on pure triglycerides like tripalmitate exhibit limited drug payloads and drug expulsion from the crystal lattice (Westesen et al., 1997). Using complex glycerides like hard fats as a matrix for SLN, incorporation of lipohilic drugs is facilitated (Siekmann, 1994). However, these hard fat SLN reveal a tendency to form supercooled melts instead of solid particles. Even if solidified at room

* Corresponding author. Tel.: +49-30-77000478; fax: +49-30-77000475.

0378-5173/00/$ - see front matter
PII: S0378-5173(00)00378-1

temperature these particles melt at body temperature. Therefore, these particles are not suited for controlled release applications. The aim of this study was to develop a nanoparticulate, lipid based drug carrier with increased payloads and controlled release properties. This was accomplished by incorporating triglyceride containing oils in the solid core of said particles.

Suppository masses are mostly comprised of semisynthetic hard fats, consisting of partial glycerides and blends of fatty acids (Coben and Lordi, 1980). Due to this inhomogeneous composition the crystal lattice structure is complex as compared to crystals formed by, e.g. monoacid triglycerides (Thoma et al., 1983). These suppository bases melt at $\sim 32–35$°C, but contain fractions of constituents which are liquid at room temperature. The amount of at room temperature liquid and solid components is described by the solid fat index (SFI). Typically, said suppositories are defined by SFIs ranking from 60 to 100%, accounting for up to 40% liquid components. These liquid components are medium chain or unsaturated fatty acids. Their structure can be defined by differential scanning calorimetry (DSC) or NMR (Müller, 1986).

The capabilities of including host molecules in the lattice of crystalline lipids are often limited whereas liquid oils normally show considerable higher solubility for lipohilic drugs. Crystalline suppository masses lack of convenient drug solubilities, even though drug solubilities can be improved by using hard fats with low SFIs (e.g. 60%). Mixtures of liquid and solid lipids are not restricted to these semisynthetic materials but can be found as well in naturally occurring products like milk, cream or cocoa butter (Precht, 1988). Similar, in this study conventional SLN were supplemented with liquid oils. It was our concept to develop a carrier with a solid matrix but liquid domains combining the advantages of the solid matrix, which prevents drug leakage, and of the liquid regions, which show comparable high solubility for lipophilic drugs. In contrast to the hard fats, a bulk material with sufficient high melting point (< 70°C) was chosen. Similar to most hard fats, the chosen Compritol 888 (glyceryl behenate) material consists of mono-, di- and triglycerides lending slight emulsifying properties to the lipid (HLB = 2). This long chain (C_{22}) glyceride was mixed with varying amounts of the medium chain triglyceride Miglyol 812 (caprylic/capric triglycerides). Other oily components like paraffin oil, 2-octyl dodecanol or isopropyl palmitate were tested as well. However, Miglyol was chosen for a broader investigation because of its chemically similar structure compared to Compritol, its good miscibility with Compritol and its good solubility for the model drug retinol. These lipid nanoparticles based on mixtures of Miglyol and Compritol were characterised by DSC, X-ray diffraction and laser diffractometry (LD). Practical implications of these manipulations were assessed by monitoring drug release in a Franz-diffusion cell type model (Franz, 1975) using a synthetic membrane.

2. Materials and methods

2.1. Materials

Compritol 888 ATO (INCI: tribehenin, US/NF: glyceryl behenate) is a mixture of ~ 15% mono-, 50% di- and 35% triglycerides of behenic acid (C_{22}) and was a gift of Gattefossé (D-Weil a. R.). Other fatty acids than behenic acid, mainly of shorter chain length, account for less than 15%. Retinol was donated by BASF (D-Ludwigshafen). Miglyol 812 (caprylic/capric triglycerides) was provided by Hüls AG (D-Witten). All other chemicals were obtained from Sigma (D-Deisenhofen).

2.2. Preparation of lipid nanoparticles and nanoemulsion

Compritol-nanoparticles were prepared as described in detail elsewhere (Müller and Lucks, 1996). Briefly, Compritol (tribehenin) was melted at 85°C and various amounts of Miglyol 812 (caprylic/capric triglycerides) and retinol were added. The hot lipid phase was dispersed in a surfactant solution and a premix was formed using an ultra turrax (IKA, D-Staufen). The premix was passed through a Lab 40 high-pressure homogeniser (APV Gaulin, D-Lübeck). Three cycles

at 500 bar and 85°C were performed. The concentrations of Miglyol and retinol were 0, 8, 16, 28, 33, 38% and 0.33, 0.8, 1.6, 2.8, 3.3, 3.8%, respectively (related to the lipid phase). The concentration of solid particles in this aqueous dispersion was 15%. A nanoemulsion was prepared in exactly the same manner only replacing Compritol by Miglyol only.

2.3. Differential scanning calorimetry

DSC was performed by a Mettler DSC 821^e (Mettler Toledo, D-Gießen). Samples containing 15 mg nanoparticle dispersions were weighted accurately in 40 μl aluminium pans. DSC scans were recorded at a heating and cooling rate of 5 K/min. Melting points and recrystallisation points correspond to the maximum and minimum, respectively, of the DSC curves.

2.4. X-ray diffraction

Wide-angle X-ray scattering (WAXS) measurements were carried out with a Nonius PDS120 powder diffractometer in transmission geometry. A FR590 generator was used as the source of CuKα radiation, monochromatization of the primary beam was achieved by means of a curved Ge crystal, and the scattered radiation was measured with a Nonius CPS120 position sensitive detector. The resolution of this detector in 2θ is 0.018°. Small-angle X-ray scattering (SAXS) measurements were recorded with an X-ray vacuum camera with pinhole collimation (Anton Paar, Austria; model A-8054) equipped with image plates (type BAS III, Fuji, Japan). The image plates were read with a MACScience Dip-Scanner IPR-420 and IP reader DIPR-420 (Japan).

2.5. Particle size analysis

Particle size analysis was performed by LD using a Malvern Mastersizer E (Malvern, UK) yielding the volume distribution of the particles. Mie analysis of the raw data was applied. A D90% value of 1 μm indicates that 90% of all particles posses a diameter of 1 μm or less.

2.6. Release study

In-vitro release studies were performed with flow-through Franz diffusion cells (0.9 cm in diameter, Crown Scientific, US-Sommerville) (Franz, 1975). The diffusion cells were thermoregulated with a water jacket at 37°C. Cellulose nitrate (0.1 μm pore diameter, Sartorius, D-Göttingen) membrane filters were soaked with isopropyl myristate to separate donor and receptor fluid (Neubert and Wohlrab, 1990) and mounted to Franz diffusion cell. Phosphate buffered saline (PBS) containing 1.5% bovine serum albumin (BSA) was used as receptor fluid. One hundred microliters of liquid nanoparticle dispersion containing retinol were applied on the donor side and covered with parafilm.

Samples were collected over 48 h and analysed with an HPLC (Kontron Instruments, D-Neufahrn) using a LiCrospher 60 RP select B 5 μm (Merck, D-Darmstadt) column, a flow rate of 1 ml/min and UV-detection at 325 nm. The limit of detection (signal/noise ratio 3:1) was 13.5 ng/ml retinol. Reproducibility was 2.1%. Data represent the arithmetic mean $\pm$ standard deviation (S.D.) ($n = 3$).

3. Results

3.1. DSC investigations

DSC gives an insight into the melting and recrystallisation behaviour of crystalline material like lipid nanoparticles. The break down of the crystal lattice by heating the sample yields inside information on, e.g. polymorphism, crystal ordering, eutectic mixtures or glass transition processes (Ford and Timmins, 1989). DSC experiments are useful to understand solid dispersions like solid solutions, simple eutectic mixtures or, as in this case, drug and lipid interactions and mixture behaviour of Compritol and Miglyol. Fig. 1 gives an overview of the melting and recrystallisation process of a 15% suspension of nanoparticles in surfactant solution. The nanoparticles were prepared with different ratios of liquid to solid lipids (different SFIs). The upper curve represents pure

Compritol SLN prepared by the hot homogenisation technique containing 0.33% retinol (related to the lipid). The next curves were recorded on lipid carriers with increasing oil amounts. The lowest curve belongs to the formulation with 38% Miglyol related to the lipid phase. For the upper curve, the melting process takes place with maximum turn over rate at 70.8°C (peak maximum). The extrapolated onset of the melting process occurs at 67.5°C. The difference between onset and maximum can be taken as a measure for the width of the peak and is in this case 3.3 K. By adding the Miglyol to the carrier, the melting point is depressed in a concentration dependent manner. At 38% oil load the melting point is depressed by almost 7 K to 63.9°C. The onset is even more influenced and dropped by almost 17 K to 50.4°C. The difference between the onset and the temperature of the maximum for these nanoparticles with the highest oil load accounts for 13.5 K indicative for massive crystal order disturbance (lattice defects). The depression of the onset and the temperature of the peak maximum depended on the oil concentration in an approximately linear fashion for the given concentration range (correlation coefficient $R^2 = 0.994$ for the onset and 0.993 for the maximum). However, the slope of the plot for the onset is more than twice the slope for the maximum temperature (-0.453 vs. -0.176 K/% oil). A similar concentration dependency was observed for the recrystallisation temperature ($R^2 = 0.994$, slope -0.155 K/% oil).

Comparing bulk raw material of Compritol and colloidal dispersions of pure Compritol the peak maximum decreased from 73.0 to 70.8 °C. This decline can be explained by the small particle size in the nanometer range, their high specific surface area and the presence of surfactants. This melting point depression can be attributed to the Kelvin effect and is described by the Thomson equation (Hunter, 1986). Additionally, an increased polymorphic transition rate has been attributed to the small particle size (Bunjes et al., 1996). Again, the increase in transition rate was explained by the small size of the crystallites (Siekmann and Westesen, 1994). The DSC experiments revealed polymorphism for Compritol nanoparticles as well. In addition to the main peak a peak shoulder at higher temperatures was observed (dark triangles in Fig. 1). Similar to the melting process the recrystallisation showed one to two peak shoulders (dark triangles). Polymorphism seemed to be more pronounced in the carriers with high Miglyol loads. However, a quantification of the

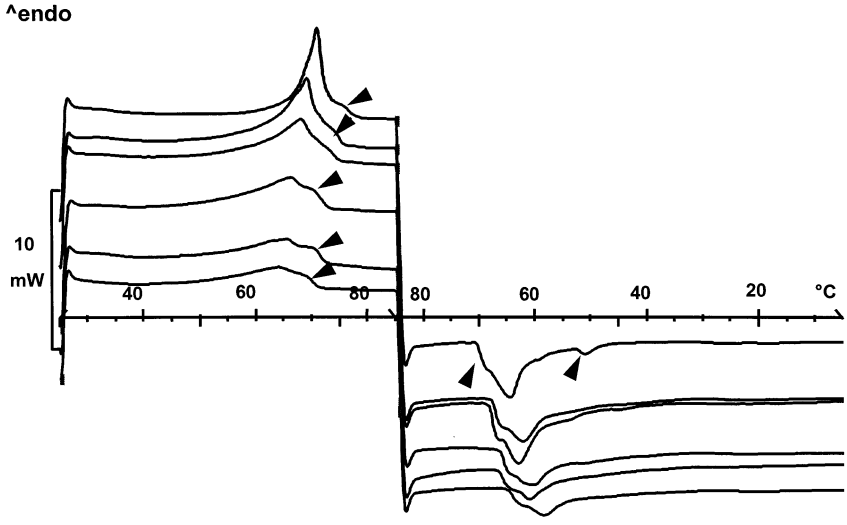

Fig. 1. DSC scans of SLN dispersions containing (from top) 0, 8, 16, 28, 33 and 38% Miglyol (heating from 25 to 85°C and subsequent cooling from 85 to 5°C at a rate of 5 K/min). Dark triangles point at minor amounts of a second (and third) polymorph of Compritol.

Table 1
Crystallisation process of a Miglyol nanoemulsion at different cooling rates (DSC data)

Cooling rate (K/min)	Onset (°C)	Maximum (°C)	Enthalpy (J/g)
2	−17.0	−25.9	9.16
5	−21.3	−29.6	7.92
10	−44.8	−47.4	6.96

two main polymorphs was not possible because of the overlapping melting and transition processes. The overall melting enthalpy for the two polymorphs was in all investigated carriers very similar (12.2, 14.3, 12.6, 14.1, 12.6 and 12.1 J/g Compritol, data shown by increasing Miglyol loads).

In addition to the characterisation of the solid material of the carrier, DSC can be employed to study the liquid phase within the nanoparticles. For this investigation, the dispersion was cooled down to −60°C and reheated up to 25°C. Upon cooling the water crystallised at −15 to −18°C. This transition was followed by the crystallisation of the Miglyol fraction. As a reference a nanoemulsion consisting of pure Miglyol was investigated. Due to the polymorphism of this triglyceride, the crystallisation temperature depended on the cooling rate. Table 1 lists the DSC characteristics of this nanoemulsion for different cooling rates. Based on this DSC data, the crystallisation temperature corresponding to the 10 K cooling rate can be attributed to the less ordered α polymorph whereas the crystallisation temperature corresponding to the 2 K rate can be assigned to the ordered β form. However, assignment of polymorphs to colloidal Miglyol emulsions needs further investigations. The following heating procedure led to the melting of the frozen Miglyol followed by the melting of the bulk water. The melting endotherm of Miglyol was very broad and interfered with the melting of water thus preventing full evaluation of this process.

Fig. 2 depicts crystallisation of Miglyol inserted in a Compritol matrix. The upper graph reveals a small exothermic event (dark triangle) at −41.2°C for the carrier with 8% oil load. In contrast the crystallisation of Miglyol in Compritol nanoparticles prepared with 16% oil (second from top) was shifted to −24.5°C but yet the enthalpy was very small. The next two graphs show 28 and 38% Miglyol load. These crystallisations exhibited a considerable exothermic event. In the case of

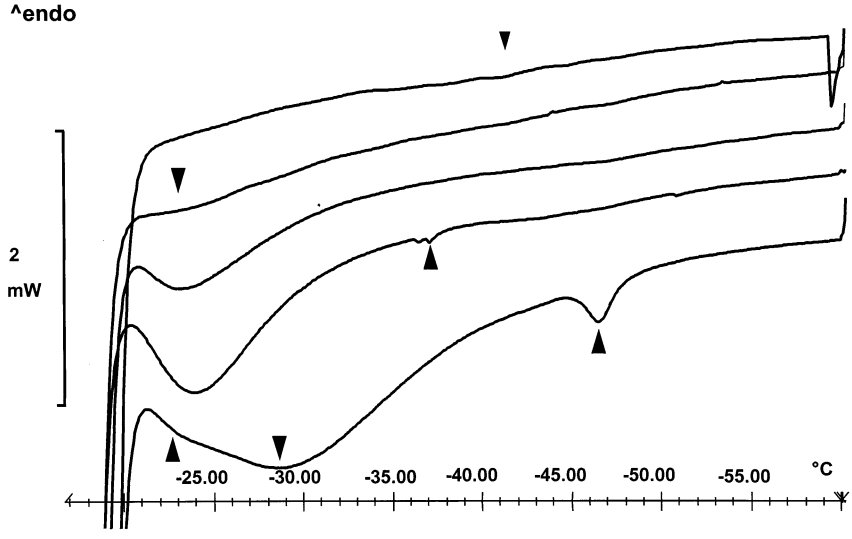

Fig. 2. DSC scans of SLN dispersions containing (from top) 8, 16, 28 and 38% Miglyol. The lowest graph represents a nanoemulsion (100% Miglyol). Cooling from 25 to −60°C at a rate of −5 K/min. Dark triangles point at different polymorphs of Miglyol.

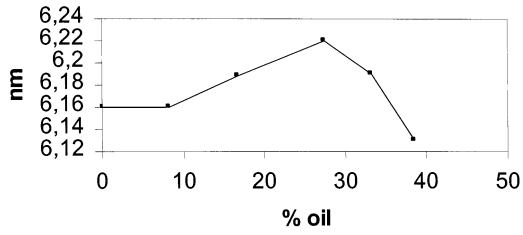

Fig. 3. Long spacings (SAXS measurements) of the Compritol lattice loaded with increasing amounts of Miglyol (% oil related to the lipid phase).

38% oil load a second small peak at -37°C appeared (dark triangle in Fig. 2). The lowest graph reflects thermal behaviour of a nanoemulsion cooled down with a rate of 5 K/min. Two peaks and one peak shoulder (dark triangles), indicating the presence of the three polymorphs α, β′ and β, were observed. The exothermic peak of this nanoemulsion was broader and more complex than the peaks resulting from the nanoparticle dispersions. The difference between onset and minimum temperature is 8.3 K in the case of the nanoemulsion and only 3.9 K for the nanoparticles with 38% oil.

The melting/crystallisation transition would be instantaneous for a theoretical 100% pure material, i.e. truly isothermal. A pure sodium chloride crystal melts almost isothermal. However, usually a melting range is observed, especially with organic substances. An increasing melting range can be correlated with impurities or less ordered crystals of, e.g. polymers. Therefore, in the case of Miglyol/Compritol nanoparticles one can conclude that the oil within the carrier should be in a higher ordered arrangement (less lattice defects, restricted polymorphism) compared to the emulsified form.

3.2. X-ray diffraction

WAXS and SAXS experiments were performed to assess the influence of the oily constituent on the subcell parameters and long spacings of the solid Compritol nanocrystals and to confirm polymorphism behaviour established by DSC measurements.

It is conceivable that the oil is inserted between the bilayer planes of the Compritol crystals (Siekmann, 1994). Such formation is however not expected since the oil is a triglyceride and thus chemically very similar favouring a homogeneous insertion of the medium chain glycerides into the long chain glycerides. Furthermore, the chain length structure, which is a repetitive sequence of acyl chains involved in a unit lamellae along the chain axis, might change from double to triple (Sato et al., 1999). These alterations in structure would lead to changes in the long spacings in a magnitude of at least ~ 0.5–1 nm. Experimentally no widening of lamellae distance of this magnitude was observed. Instead long spacings varied within 0.1 nm (Fig. 3). Furthermore, no linear relation between oil concentration and long spacing was observed. Thus, insertion between the lamellae and transition from double to triple chain length structure is unlikely.

WAXS measurements are useful to determine the subcell parameters and thus the polymorphic form of the glycerides. According to Larsson short spacings of triglycerides can be described as following (Larsson, 1966):

- α: hexagonal (H) subcell with a lattice spacing of 0.42 nm
- β′: orthorhombic perpendicular ($O_{\perp}$) subcell with strong lattice spacings of 0.42–0.43 and 0.37–0.40 nm
- β: triclinic parallel ($T_{//}$) subcell with a strong lattice spacing of 0.46 nm.

Further polymorphic forms are found with complex glycerides like mixed acid triacylglycerides or partial glycerides. Multiple β′ and β, sub α or intermediate forms were described (Sato et al., 1999). Nevertheless, nomenclature and properties of monoacid triglycerides can also be used for these complex glycerides that have similar crystal packing (Hagemann, 1988). Because of the basic resemblance of the lipid mixture presented here and hard fats, the concept of an intermediate β_i form presented by Precht (1988) is adopted for this study.

Table 2 shows the short spacings for Compritol bulk material and mixtures of Compritol bulk and Miglyol prepared by melting two parts Compritol with one part Miglyol at 85°C and subsequent

cooling. The mixtures contained either no or 3.3% retinol. Whereas the pure Compritol exhibited the β′ form, the addition of Miglyol led to a bulk material probably consisting of β′ and smaller amounts of β_i. It is well known that the introduction of short or medium chain components generally accelerates the rate of polymorphic transition, which can be observed here as well. The presence of retinol seems to reduce this transition process of the bulk material, which was not expected.

Fig. 4 reveals the WAXS diffractograms of Compritol nanoparticles loaded with (from top) 38, 33, 16, 8 and 0% oil. The pure Compritol SLN (lowest graph, no oil supplement) revealed a diffraction pattern very similar to that of the bulk material thus being in the β′ state. A small third peak at 0.46 nm arose with increasing oil concentration (arrow) indicating the (partial) formation of β_i. It seems not possible to clearly identify β′ or β_i or mixtures thereof by their short spacings shown in this diagram. Usually different polymorphs display different long spacing as well. A mixture of two polymorphs leads to two distinguishable long spacings. Therefore, it should be possible to differentiate between β′ and β_i and mixtures thereof by their long spacings. However, in the special case of β′ and β_i no such differences in long spacing can be detected and thus no further information on this special polymorphism can be derived. Even without clear nomenclature, one can conclude that the oil has a measurable impact on the crystal ordering by favouring formation of an intermediate β form.

Table 2
Characteristic short spacings of different bulk material: pure Compritol, Compritol with 33% Miglyol and Compritol with 33% Miglyol and 3.3% retinol

Bulk material	Short spacings (nm) (relative intensity, %)	Polymorph
Compritol	0.417 (100) 0.380 (32)	β′
Compritol + Miglyol	0.414 (100) 0.372 (51) 0.456 (16)	β′ and/or β_i
Compritol + Miglyol + retinol	0.417 (100) 0.370 (40) 0.458 (8)	β′ and/or β_i

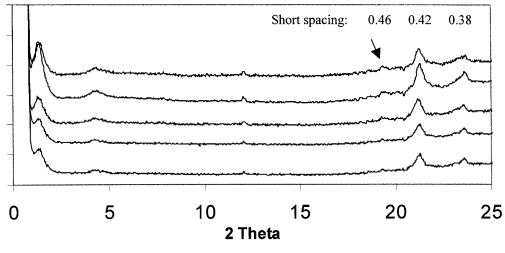

Fig. 4. WAXS diffraction pattern of SLN dispersions with (from top) 38, 28, 16, 8 and 0% Miglyol. The arrow points at a small third peak arising at 0.46 nm with higher oil loads.

3.3. Particle size analysis

Nanoparticle dispersions were prepared by high pressure homogenisation at elevated temperatures. A sufficient high energy input is necessary to break down the droplets into the nanometer range (Schwarz et al., 1994). A finer dispersion can be obtained by increasing the production temperature, pressure or the number of homogenisation cycles. Maximum dispersity is reached after a certain energy input. Further energy input does not improve or even worsen the result with respect to a small size and narrow size distribution. Besides production parameters, lipid matrix, surfactant blend and viscosity of lipid and aqueous phase influence the outcome of the procedure (Müller et al., 1993). Leaving all other parameters constant, in this study the only variable was composition of lipid matrix varying from no oil load to 38% oil load. A lipid phase of low viscosity can be dispersed more easily and thus the viscosity has an influence on particle size. The viscosities of Miglyol and Compritol mixtures at different temperatures were studied in (Fischer-Carius, 1998). It was shown that the viscosity at 85°C of pure Compritol and Compritol/Miglyol mixtures were low ($\sim$ 1.5 mPa s) and very similar. Around the melting point of Compritol (73°C) and below clear differences can be seen. Below 70°C viscosity of Compritol increases rapidly

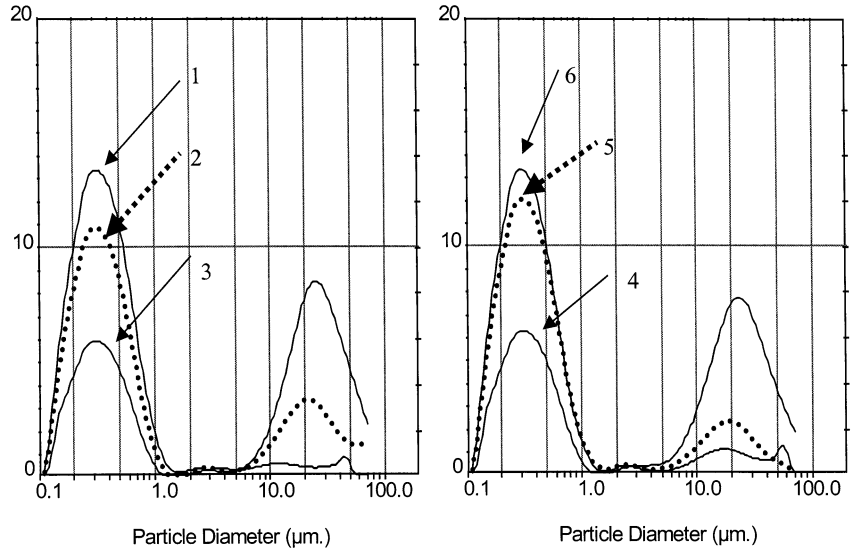

Fig. 5. Particle size measurements (LD, volume distribution in %) on SLN dispersions stored for 3 months at room temperature. (1) 0, (2) 8, (3) 16, (4) 28, (5) 33 and (6) 38% oil load.

whereas the addition of 30% Miglyol lowered the slope of the increase (e.g. at 60°C: >100 mPa s pure Compritol, 5 mPa s Compritol with 30% Miglyol). From these data relevant impact of viscosity on the homogenisation process at 85°C seems likely only for an incompletely thermoregulated homogeniser with colder spots. In these cases the addition of a low viscous oil improves the size distribution.

Compritol is a partial glycerides with 15% mono- and 50% diglycerides. It was suggested (Westesen et al., 1993) that these surface active partial glycerides facilitate emulsification and form more rigid surfactant films and therefore improve long term stability. Replacing Compritol by the triglyceride Miglyol, the percentage of mono- and diglycerides of the carrier is reduced. In the case of a 38% oil load the content of mono- and diglycerides is reduced to 9.3 and 31%, respectively. Thus increasing oil loads should tend to broaden size distribution and reduce long term stability.

LD measurements performed 1 day after production revealed basically similar sizes and size distributions with D50% around 0.35 μm and D90% around 0.80 μm for all lipid nanocrystal suspensions. The immediate influence of oily constituents on the production process was, as expected, obviously low. In contrast, measurements performed 3 months after production depicted quite different long-term stabilities. Whereas the nanoparticles with no oil (one) and 38% (six) oil showed sufficient long-term stability with only slight particle growth, the intermediate concentrations resulted in considerable aggregation (Fig. 5).

3.4. Drug release

Drug release was studied using Franz diffusion cells separating the receptor fluid and the nanoparticle dispersion with a lipophilic membrane. The diffusion process through the membrane is most often lead by the thermodynamic activity c/c_s, showing linear increasing diffusion rates with increasing thermodynamic activities (Bendas et al. 1995). For a given vehicle the concentration c of a drug within the vehicle can be used instead of thermodynamic activity because the saturation solubility c_s is constant. In the case of the tested different nanoparticles and nanoemulsions the saturation solubility is not constant but varying. Due to experimental difficulties the saturation concentration of retinol in lipid nanocrystals can not be measured directly.

Instead, c_s was calculated by addition of the solubilities in Miglyol and in solid Compritol. The solubility of retinol in Miglyol at room temperature was determined to be 26% and the solubility in solid Compritol was roughly 1%. The saturation solubility of retinol in the droplets of the nanoemulsion was, therefore, 26% and, for example, of the carrier comprising 38%, oil 10.5%.

Table 3 lists the amounts of retinol released after 2, 24 and 48 h. Data are based on either concentrations or activities and expressed as percent of the applied dose or activity respectively. Best controlled release was demonstrated for the particles with low oil amounts. At 2 h the effects were most significant. From the thermodynamic point of view, the controlled release formulations delayed drug release by a factor of at least four and up to 56-fold for this period of observation. After 24 h and even more after 48 h similarity between nanoparticles and nanoemulsion increased. For the cumulated drug release after 48 h the released amount of retinol was only 1.5-fold lower for the carrier with higher oil loads than for the nanoemulsions. Yet a factor of four remained for the lipid particles with no or low oil loads.

4. Discussion

SLN based on hard fats were prepared by Siekmann (1994) because of their higher solubility for lipophilic drugs like oxazepam or menadione. A content of partial glycerides and liquid fractions favours successful drug inclusion and avoids drug expulsion as described for pure triglycerides like tripalmitate (Westesen et al., 1997). Despite the advantages of complex glycerides and less ordered crystal packing, hard fat SLN possess a number of clear disadvantages as well. Due to their low melting point and complex composition, the recrystallisation after production by hot homogenisation technique is considerably retarded. Because these particles do not always solidify at room temperature, emulsions of supercooled melts rather than solid suspensions can be observed. These supercooled melts can not immobilise drugs in the same way as crystalline nanoparticles, thus controlled release can not be achieved with these carriers (Bunjes et al. 1996). Even though recrystallisation of these particles can be improved by storage at refrigerated temperatures, controlled release of these solid hard fat particles is faint because they melt at body temperature.

The aim of this study was to develop a nanoparticulate system with increased drug loading capacity similar to hard fat SLN and controlled release similar to crystalline nanoparticles. Based on the solubility properties of many lipophilic drugs, which show high or sufficient solubility in liquid oils but poor solubility in solid triglycerides, we combined liquid and solid lipids to form a homogenous solid carrier with liquid nanocompartments. Miglyol 812 was chosen because of its good solubility properties and its chemical structure. Compritol shows a sufficiently high melting point and prevents melting of the particle at body temperature. DSC measurements showed that both components exhibit good miscibility in the nanoparticulate state and formed

Table 3
Cumulative drug release expressed as percent of the applied dose (C) and activity (A)[a]

Oil load		0%	8%	16%	28%	38%	100%
C	2 h	0.45 ± 0.2	0.91 ± 0.3	1.12 ± 0.1	5.51 ± 0.7	5.48 ± 0.5	7.45 ± 0.6
	24 h	6.05 ± 0.5	6.64 ± 1.3	23.5 ± 1.5	40.0 ± 5.1	27.5 ± 0.9	15.2 ± 0.8
	48 h	24.1 ± 2.2	19.1 ± 5.3	45.9 ± 0.8	54.5 ± 2.9	45.6 ± 4.6	22.3 ± 2.5
A	2 h	0.41 ± 0.2	0.67 ± 0.2	0.99 ± 0.1	5.33 ± 0.7	5.48 ± 0.5	22.4 ± 1.8
	24 h	5.52 ± 0.5	4.90 ± 1.0	20.8 ± 1.3	38.7 ± 4.9	27.5 ± 0.9	45.6 ± 2.4
	48 h	22.0 ± 2.0	14.1 ± 3.9	40.5 ± 0.7	52.7 ± 2.8	45.6 ± 4.6	66.9 ± 7.5

[a] Arithmetic means ± S.D. ($n = 3$).

homogenous particles. Because the melting point of Compritol was depressed and peak width was broadened in an oil concentration manner, phase separation could be excluded. Since the peak width was more affected than the peak maximum, a certain phase separation within one particle can be assumed.

Freezing experiments have revealed liquid oil regions (nanocompartments) crystallising at ~ -25°C. The slope of the crystallisation peak was higher for oil inside a nanoparticle compared to the nanoemulsion of Miglyol. Thus, the inclusion of the oil in Compritol cavities led to a higher ordered yet liquid state of the molecules. A reduced mobility for these molecules can be demonstrated by ^{1}H-NMR spectroscopy as well (unpublished data). Small oil concentrations (8–16%) led to a probable predominantly random distribution of oil molecules replacing Compritol molecules of the crystal lattice. Thus no or only very little crystallisation enthalpy was set free. Higher concentrations of Miglyol led to well detectable peaks in the DSC run pointing at cluster formation. Exact determination of the arrangement of Miglyol molecules inside the Compritol particle was beyond the scope of the present study.

Further structural information was derived from SAXS and WAXS analysis. Overall arrangement of the glyceride molecules was not affected by the presence of oil. Double chain structure was preserved and short spacing varied within 0.1 nm. Variations of these magnitude can be observed for binary mixtures of two solid lipids as well (Bunjes et al., 1996) and probably result from the different chain lengths of the components. No linearity between oil concentration and long spacing was observed, instead a maximum occurred for 28% oil load. Increasing bilayer thickness demonstrated a more loosely packing. Addition of the pure triglyceride Miglyol to the partial glyceride Compritol reduced the relative impact of free hydroxy groups on the long spacing. Whereas pure Compritol is mainly a diglyceride, in nanoparticles with 38% Miglyol the triglyceride fraction predominates. Bilayer thickness of monoglycerides is constant in all polymorphic forms underlining the strong influence of the polar region on the structure (Hernqvist, 1988). The SAXS patterns with only one peak suggest that one mixed crystalline particle containing both components, and not two crystal populations, are formed. Because all SAXS reflections showed similar line width, the crystal lamellae order was less effected by oil supplementation.

WAXS additionally revealed similar polymorphic behaviour of the tested carriers. A slightly increased polymorphic transition rate was observed for SLN with higher oil loads. Partial formation of β_i was detected in these cases. A higher transition rate was further evidenced by DSC measurements on samples stored for 3 months (data not presented).

Long term physical stability as measured by particle size analysis can be discussed with regard to the structural information mentioned above and varying amounts of partial glycerides present in the water/lipid interface. Best long-term stability can be obtained with no or high oil concentrations. The high fraction of mono- and diglycerides in the carrier of pure Compritol is made responsible for its good long-term stability. The highly disordered state in Compritol nanoparticles with 38% Miglyol delays recrystallisation and thus improves physical stability (Westesen et al. 1997).

All investigated drug carrier formulations displayed controlled drug release, with low oil loads showing the most sustained release. With increasing oil concentration similarity to the release pattern of an emulsion became more evident. We conclude that the presented concept of mixing liquid and solid lipids successfully circumvents limited drug loads of conventional SLN (0.33% retinol in conventional SLN as compared to 3.8% for Compritol/Miglyol nanoparticles). However a partial loss of controlled release properties must be taken into account. No linear relation between oil concentration and many structural parameters and release rate was observed. Thus each oil concentration leads to a distinguishable lipid based drug carrier. These novel lipid particles containing liquid nanocompartments (nanocompartment carrier, NCC) seem to be well suited for dermatological applications since sufficient amounts of less potent drugs can be encapsulated. Furthermore, a controlled drug release over sev-

eral hours is sufficient for certain dermal formulation (Embil and Nacht, 1996) which can be achieved with this novel lipid carrier suspensions.

References

Bendas, B., Schmalfuß, U., Neubert, R., 1995. Influence of propylen glycol as cosolvent on mechanisms of drug transport from hydrogels. Int. J. Pharm. 116, 19–30.

Bunjes, H., Westesen, K., Koch, M.H.J., 1996. Crystallization tendency and polymorphic transitions in triglyceride nanoparticles. Int. J. Pharm. 129, 159–173.

Coben, L.J., Lordi, N.G., 1980. Physical stability of semisynthetic suppository bases. J. Pharm. Sci. 69, 955–960.

Embil, K., Nacht, S., 1996. The microsponge delivery system: a topical delivery system with reduced irritancy incorporating multiple triggering mechanisms for the release of actives. J. Microencapsulation 5, 575–588.

Fischer-Carius, A., 1998. Untersuchungen an extrudierten und sphäronisierten Matripellets mit retardierter Wirkstoffabgabe. PhD Thesis, FU Berlin, Germany.

Ford, J.L., Timmins, P., 1989. Pharmaceutical Thermal Analysis. Ellis Horwood, Chichester.

Franz, T.J., 1975. Percutanous absorption. On the releveance of in vitro data. J. Invest. Dermatol. 67, 190–196.

Hagemann, J.W., 1988. Thermal behaviour and polymorphism of acylglycerides. In: Garti, N., Sato, K. (Eds.), Crystallization and Polymorphism of Fats and Fatty Acids. Marcel Dekker, New York, pp. 9–95.

Hernqvist, L., 1988. Crystal structures of fats and fatty acids. In: Garti, N., Sato, K. (Eds.), Crystallization and Polymorphism of Fats and Fatty Acids. Marcel Dekker, New York, pp. 97–137.

Hunter, R.J., 1986. Foundations of Colloid Science, vol. 1. Oxford University Press, Oxford.

Larsson, K., 1966. Classification of glyceride crystal forms. Acta Chem. Scand. 20, 2255–2260.

Müller, B.W., 1986. Suppositorien. APV Monographie, Wissenschaftliche Verlagsgesellschaft mbH Stuttgart.

Müller, R.H., Lucks, J.S., 1996. Arzneistoffträger aus festen lipidteilchen — feste lipid nanosphären (SLN). European patent EP 0 605 497 B1.

Müller, R.H., Schwarz, C., Mehnert, W., Lucks, J.S., 1993. Production of solid lipid nanoparticles for controlled drug delivery. Proc. Int. Symp. Control. Rel. Bioact. Mater. 20, 480–481.

Neubert, R., Wohlrab, W., 1990. In-vitro methods for the biopharmaceutical evaluation of topical formulations. Acta Pharm. Technol. 36, 197–206.

Precht, D., 1988. Fat crystal structure in cream and butter. In: Garti, N., Sato, K. (Eds.), Crystallization and Polymorphism of Fats and Fatty Acids. Marcel Dekker, New York, pp. 305–355.

Sato, K., Ueno, S., Yano, J., 1999. Molecular interactions and kinetic properties of fats. Prog. Lipid Res. 38, 91–116.

Schwarz, C., Mehnert, W., Müller, R.H., 1994. Influence of production parameters of solid lipid nanoparticles (SLN) on the suitability for intravenous injection. Eur. J. Pharm. Biopharm. 40, 24S.

Siekmann, B., 1994. Untersuchungen zur Herstellung und zum Rekristallisationsverhaltern schmelzemulgierter intravenös applizierbarer Glyceridnanopartikel. PhD Thesis, TU Braunschweig, Germany.

Siekmann, B., Westesen, K., 1994. Thermoanalysis of the recrystallization process of melt-homogenized glyceride nanoparticles. Colloids Surf. B 3, 159–175.

Thoma, K., Serno, P., Precht, D., 1983. Röntgendiffraktometrischer nachweis der polymorphie von hartfett. Pharm. Ind. 45, 420–425.

Westesen, K., Siekmann, B., Koch, M.H.J., 1993. Investigations on the physical state of lipid nanoparticles by synchrotron X-ray diffraction. Int. J. Pharm. 93, 189–199.

Westesen, K., Bunjes, H., Koch, M.H.J., 1997. Physicochemical characterisation of lipid nanoparticles and evaluation of their drug loading capacity and sustained release potential. J. Controlled Release 48, 223–236.